Eur. Phys. J. B **28**, 81–89 (2002)
DOI: 10.1140/epjb/e2002-00203-1

THE EUROPEAN PHYSICAL JOURNAL B

Switching current noise and relaxation of ferroelectric domains

B. Tadić[a]

Jožef Stefan Institute, PO Box 3000, 1001 Ljubljana, Slovenia

Received 7 February 2002 / Received in final form 10 April 2002
Published online 9 July 2002 –

Abstract. We simulate field-induced nucleation and switching of domains in a three-dimensional model of ferroelectrics with quenched disorder and varying domain sizes. We study (1) bursts of the switching current at slow driving along the hysteresis loop (electrical Barkhausen noise) and (2) the polarization reversal when a strong electric field was applied and back-switching after the field was removed. We show how these processes are related to the underlying structure of domain walls, which in turn is controlled by the pinning at quenched local electric fields. When the depolarization fields of bound charges are properly screened we find that the fractal switching current noise may appear with two distinct universal behaviors. The critical depinning of plane domain walls determines the universality class in the case of weak random fields, whereas for large randomness the massive nucleation of domains in the bulk leads to different scaling properties. In both cases the scaling exponents decay logarithmically when the driving frequency is increased. The polarization reverses in the applied field as a power-law, while its relaxation in zero field is a stretch exponential function of time. The stretching exponent depends on the strength of pinning. The results may be applicable for uniaxial relaxor ferroelectrics, such as doped SBN:Ce.

PACS. 77.80.Dj Domain structure; hysteresis – 77.80.Fm Switching phenomena – 05.40.Ca Noise

1 Introduction

Polarization reversal and properties of the accompanying switching current are relevant for various applications of ferroelectric materials. In particular, it is a key process that takes place in electronic devices based on ferroelectrics thin films, where a reproducible switching process is required. Apart from the extensive experimental and theoretical work [1–3], a complete understanding of the domain-wall motion and predictability of the switching processes remains elusive in real ferroelectrics, especially when several physical parameters, determining either structure or dynamics, are varied. Domain switching and relaxation (back-switching) in ferroelectrics can be studied by hysteresis loop, switching current, and switching current bursts (electrical Barkhausen noise).

The development of domain structure and motion of domain walls during switching can be regarded in the scope of nonlinear dynamic processes occurring in driven disordered systems, which are studied extensively in the past decade. Particularly, the measurements on ferromagnets (a short review is given in [4]) show that Barkhausen noise exhibits interesting fractal properties, that can be characterized by a full set of scaling exponents of the sizes, durations and energies of the bursts and of the power spectrum. An example with a complete set of measured scaling exponents and corresponding fractal dimensions with derivation of the associated scaling relations can be found in reference [5]. A possible grouping of the scaling exponents into different universality classes of scaling behavior offers a new and simple link between the measured Barkhausen noise and the domain structure. For example, in a recent study [6] such a relation was established between the universal scaling exponents of acoustic emission noise and the packing properties near the first-order structural transformation.

The electrical Barkhausen noise has been observed experimentally in $BaTiO_3$ [1,2,7] and $Gd_2(MoO_4)_3$ and $LiTaO_3$ [8,9] single crystals and in $9.4/65/35(Pb,La)(Zr,Ti)O_3$ (PLZT) ceramics [10] and $PbMg_{1/3}Nb_{2/3}O_3$ (PMN) relaxor ferroelectric [11]. Physically, the polarization reversal and domain wall motions in ferroelectrics is accompanied with the local change of sign of bound charges, which influences values of the electric field in the sample. The depolarization field of bound charges can be partially screened by an adequate addition of charges on the surface and by other methods (see [3] and references therein). Hence at a given point x in the sample at time t un-compensated depolarization field is given by [3]

$$\delta E_{dep}(x,t) = E_{dep}(x,t) - \sum E_{sreen}(x,t), \qquad (1)$$

where $\sum E_{sreen}(x,t)$ is a total field due to screening (surface and bulk) charges at that site. Incomplete screening of the depolarization field tends to change the electric field

[a] e-mail: Bosiljka.Tadic@ijs.si

inside the sample, thus influencing the course of switching process itself. For instance, there is a finite probability that inverse jumps of polarization (negative Barkhausen pulses) [1,3] occur, that slow down the switching. Recently a series of sophisticated measurements were done [9,12] that reveal the effects of the depolarization field on a created plane domain wall in $Gd_2(MoO_4)_3$ and on a multidomain structure in $LiTaO_3$. The obtained distributions of lengths, sizes and rest time of Barkhausen jumps obey a power-law behavior with an exponential cut off, both for switching and back-switching processes. Using a suitable experimental set-up the power-spectrum in PMN relaxors was measured, which was found to decay with frequency ω as $S(\omega) \sim \omega^{-2}$ [11].

Recently studied uniaxial relaxor ferroelectrics $Sr_{0.61}Ba_{0.39}Nb_2O_6$ (SBN61) and $Pb_{0.61}Ba_{0.39}Nb_2O_6$ are regarded as systems with the Ising symmetry of the order parameter, having the tetragonal structure in the low-temperature phase with the spontaneous polarization along c-axis [13,14]. In solid solutions SBN61: X doping with $X = Ce^{3+}$, Cr^{3+}, Co^{2+} reduces the transition temperature and induces local electric random fields, which give rise to local polar clusters [14]. Recently a comprehensive series of measurements in SBN: Ce and similar systems [13–15] gave a strong support to the presence of random electric fields in this class of relaxor ferroelectrics. In general, more common sources of uncorrelated random fields in ferroelectrics are neutral defects that can locally break the polar symmetry, as for instance in TGS (see detailed discussion in Ref. [16], page 149). Note that, in contrast to ferroelectrics, in ferromagnets local random fields are not allowed by the symmetry, but are theoretically constructed as being induced by coarse graining due to other types of disorder (see also [17]).

In this work we simulate temporal behavior of polarization driven by the electric field in three-dimensional systems of Ising spins subject to *quenched* local random fields and positive nearest-neighbor interaction, which is compatible with the occurrence of a ferroelectric long-range order. We consider two types of driving. First, by stepwise increase (decrease) of the external field along a hysteresis loop (see below) we study bursts in the switching current $j(t) = \mathrm{d}P(t)/\mathrm{d}t$ (electrical Barkhausen noise). We discuss effects of incomplete screening of depolarization fields on the coarse of switching and hysteresis loop properties. When the screening is complete, we study how the statistical properties of the noise depend on the strength of pinning and on the frequency with which the driving field is changed. Second, by imposing a high opposite value of the external field in the homogeneous state we let the polarization to reach its saturation at that field, and then remove the field. We determine reversal and spontaneous back-switching of the polarization with time at different strength of disorder. This type of switching is more familiar in the experiments on ferroelectrics [15].

Apart from allowing negative Barkhausen pulses as described below, the present study is complementary compared to earlier simulations of Barkhausen pulses in 3-dimensional Ising systems in the presence of disorder [18–21] in the following sense: In the earlier work [18] we considered only strong disorder that is compatible with nucleation of small domains under driving field, as for instance in relaxor ceramics, and analyzed the signal from only central part of the hysteresis loop, as it is usually done on experiments. In the present work the study is extended to entire range of disorder including the weak pinning region where extended domain walls may occur due to lack of pinning centers [22]. In this case a potential depinning of domain walls at a critical driving field contributes significantly to the scaling behavior of Barkhausen pulses, as recent theoretical results on Bethe lattice suggest [23]. Therefore, we include integration over entire hysteresis loop in order to incorporate the contribution of critical depinning to the universal scaling properties of the induced electrical noise in the case of weak pinning [24]. Furthermore, here we employ the *simulation algorithm at finite driving rates*, that mimics closely the experimental situation with stepwise increase (decrease) of the electric field. We examine in detail the effects of driving rates in both strong and weak pinning case by varying height of the steps in the external field. The earlier simulations in references [19,20] were done in the limit of zero driving rate, which appears physically inaccessible to real experiments. Whereas an entirely different aspect concentrating on the dynamic scaling during the growth of *individual* avalanches was considered in [21]. It should be stressed that in this paper we implement strictly *quenched disorder*, as described in Section 2. Note that some speed algorithms, as for instance used in [20,21], allow certain dynamic variations of pinning while the avalanche grows, which can be relevant to systems with annealed rather than quenched disorder. Theoretically, having unfixed pinning centers during the avalanche growth may alter the long-range correlations in the avalanche-triggering fields and in distances between initial points of avalanches, which were shown to be closely associated with the appearance of the fractal noise in two-dimensional systems [25].

The paper is organized as follows. In Section 2 we introduce the model and discuss all relevant parameters that influence the hysteresis loop properties. In Section 3 we study in detail scaling behavior of the switching current noise under varying disorder and driving conditions. Section 4 contains the results of switching in a high field and spontaneous back switching of polarization when the pinning is varied. The paper contains a short summary of the results and discussion in Section 5.

2 Model and relevant parameters

We consider a model with Ising-type spins situated on three-dimensional simple cubic lattice with positive interactions between neighbor spins and local random field at each lattice site [17]:

$$\mathcal{H} = -\sum_{x,y} J_{xy} S(x) S(y) - \sum_{x} h_x S(x) - E \sum_{x} S(x). \quad (2)$$

We assume that the random exchange interactions $J_{x,y}$ are distributed around a positive value J with a narrow distribution. The random fields h_x are given by Gaussian distribution with zero mean and the width f (measured in units of J^2). As mentioned above, the source of local random fields can be neutral defects that break polar symmetry [16] or charge disorder due to doping [14], which cause occurrence of polar regions in relaxor ferroelectrics. In addition, a random part of the interaction between these polar regions contributes to the observed glassy behavior of the dielectric response [26]. Since the random fields locally break the symmetry of the order parameter, we believe that the dominant disorder effects on the dynamics that we consider are due to random fields. Therefore, here we neglect the randomness in the spin-spin interaction.

The spin dynamics that we are considering is field-assisted and takes part deeply in the ordered phase. Hence, we neglect possible temperature effects, both for the reasons of keeping the number of parameters finite and assuming that they play a secondary role in these processes. The dynamics consists of spin alignment along a locally dominant field. Thus, when the local field at site x and time t, $h_{loc}(x,t)$ exceeds zero, the spin $S(x,t)$ at that site flips and thus aligns along the local field. The local field $h_{loc}(x,t)$ consists of the interaction and pinning part $h_{ip}(x,t) = \sum_y J_{xy}S(y,t) + h(x)$ and the driving field $E(x,t)$. The driving field itself is given by $E(x,t) = E_{ext}(t) - \delta E_{dep}(x,t)$, where $E_{ext}(t)$ is the external field and $\delta E_{dep}(x,t)$ a non-compensated part of the depolarization field at that site [3]. We employ a slow stepwise increase of the external field $E_{ext}(t_i) = -E_{sat} + t_i \Delta E$ at discrete time intervals $\{t_i\}$, while assuming that a non-compensated part of the depolarization field at site x may assist a probabilistic (probability parameter b) back-flip of an already aligned spin at that site. It should be stressed that the parameter b represents the probability that at a site x in time t the depolarization field opposes the effect of external filed. (The situation where the depolarization field is parallel to the external field is less interesting within the present numeric implementation of the dynamics where driving rate is not fixed, as described below.) Having in mind that the depolarization field at a given site depends on the actual domain structure and its kinetics, the uniform distribution of the stochastic variable b can be regarded only as a first step towards modeling of this complex phenomena.

Implementation of the dynamics is as follows: Quenched random fields of Gaussian distribution (in double precision) are generated and stored. They are *kept constant until entire hysteresis loop is completed* by the driving field. The external field is increased by a small amount ΔE and the set of local fields $\{h^{loc}(x,t)\}$ computed at each lattice site and stored. The system is updated *in parallel*, *i.e.*, with respect to stored set of local fields, and the spin flipped when $h^{ip}(x,t) + E_{ext}(x,t)$ exceeds zero by a small amount 10^{-10}. When it is assumed that the depolarization field is not entirely compensated, the spin flip is executed with a reduced probability $1-b$. This completes one time step of avalanche evolution. Then a new set of local fields at affected sites (neighbors of just flipped spins) is computed and stored. The conditions for spin flips at those sites examined and spins flipped according to the above rule. The process continues until no more spins are found which satisfy the conditions for flip. This completes one Barkhausen avalanche. Then the external field is increased again by the amount ΔE. When the whole loop is completed, we set another distribution of quenched random fields and repeat the driving. The results are averaged over the entire ensemble (up to 200) of different random-field realizations.

In this model the following relevant parameters appear: Width of the random-field distribution f, that determines strength of pinning and/or domain size; jump ΔE of the external field, which defines the driving rate; probability of back-flips b, which is related to the unscreened part of the depolarization field. In practice, usually an additional parameter is due to the section of the hysteresis loop at which the signal is monitored, since the properties of the signal vary along the loop. As mentioned above, here we integrate the statistics over the entire hysteresis loop in order to capture the contribution of the depinning of large domain walls to the scaling behavior of noise by weak pinning.

The hysteresis loop dependence on pinning by random fields and on driving rates is shown in Figure 1. By varying the strength of pinning f the form of the hysteresis loop changes (Fig. 1a) from the rectangular loop at low disordered 3-d sample to the slim loop, when the pinning is strong (large f). In the case of low disorder, *i.e.*, at weak pinning of domain walls, large domains may form due to lack of pinning centers. In real ferroelectrics occurrence of large domains are usually accompanied by extended plane domain walls [7,8,22]. On the other side, when the pinning is strong, such as in the case of pinning at grain boundaries of small grain ceramics [10], many small domains can be nucleated at spatially distributed centers with weak pinning, and their walls can propagate along few active sites with weakest pinning, as the driving field increases. This makes effectively low-dimensional walls moving in a three-dimensional sample. In addition, a massive nucleation of domains in the central part of hysteresis imposes a spatial restriction on the growth of later domains. Hence we expect a different scaling behavior of sizes and durations of induced switched domains in the case of weak and strong disorder. Our simulations confirm this phenomenological picture. In ferroelectrics a continuous variations of the size of domains can be achieved by increasing temperature or by applying stress, as for instance described in 8/65/35 PLZT ceramics [27]. It was suggested in reference [15] that the appropriate illumination of samples can notably reduce the strength of pinning in doped relaxor SBN61: Ce^{3+} ferroelectrics.

We would like to stress that in the algorithm keeping the external field constant during the avalanche evolution and increasing it only *after* the avalanche has stopped does not allow to study rest periods between avalanches. However, this type of field update leads to a better resolution of the noise, while it changes the time dependence of the

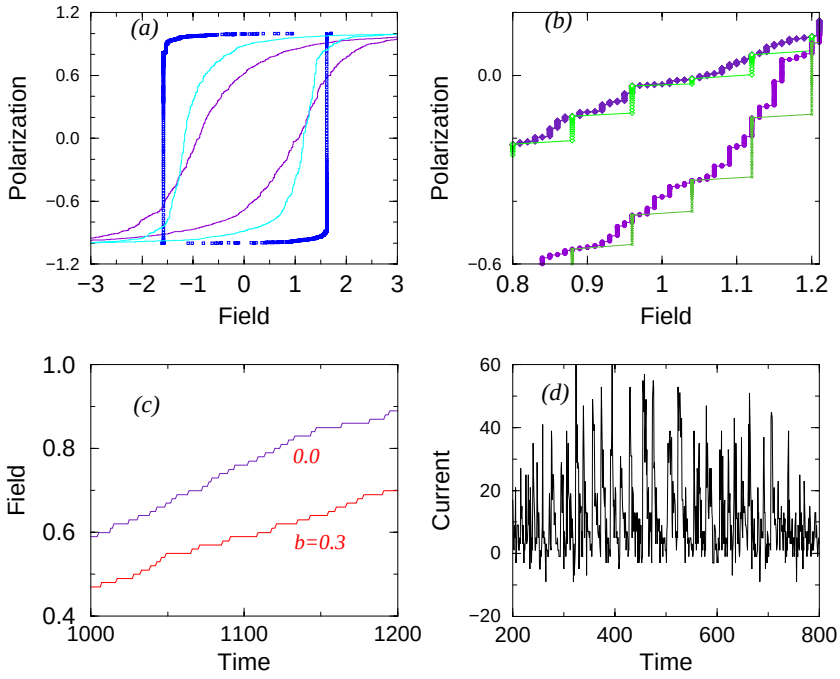

Fig. 1. (a) Hysteresis loop for driving rate $r \equiv \Delta E/J = 0.01$ and varying strength of disorder $f = 4$, 3.2, and 2 (inside out). (b) Sections of the first two loops from (a) for two different driving rates $r = 0.01$ (dark) and $r = 0.08$ (clear symbols). (c) Variation of the driving field with time and (d) the electrical Barkhausen noise (switching current) for finite probability of back flips $b = 0.3$. Figure 1 from reference [18].

driving field (*cf.* Fig. 1c). The driving rate can be better defined as the average derivative $r \equiv \langle \mathrm{d}E(t)/\mathrm{d}t \rangle$ along the loop. In the simulations we find that when back flips occur with a finite probability $b > 0$ they effectively reduce increase of the driving field and prolong the duration of a jump, as well as inducing inverse jumps, as shown in Figure 1c, d.

Assuming that the back flips occur very rarely ($b \to 0$), we obtain the switching current noise which is shown in Figure 2. The train of bursts of the switching current exhibits a long-range correlations – Fourier spectrum $j(\omega)$ of the signal is shown in Figure 2 (top). It is related to the power-spectrum *via* $S(\omega) = |j(\omega)|^2$, that can be directly measured (see [11]). Hence, the exponent of the power spectrum in the present model is given by $2 \times \phi = 1.48 \pm 0.02$ for the case of moderate pinning $f = 3.6$. The power-law behavior of the power spectrum suggests that the switching current noise exhibits fractal character when certain conditions are met, in particular, when the depolarization fields are successfully screened.

3 Fractal properties of the switching-current noise

The fractal noise of the switching current have a range of universal scaling properties, that can be determined more clearly if the field inside the sample is fully controlled. Therefore, in this section we put $b = 0$ in order to study in detail these scaling properties and to determine how they

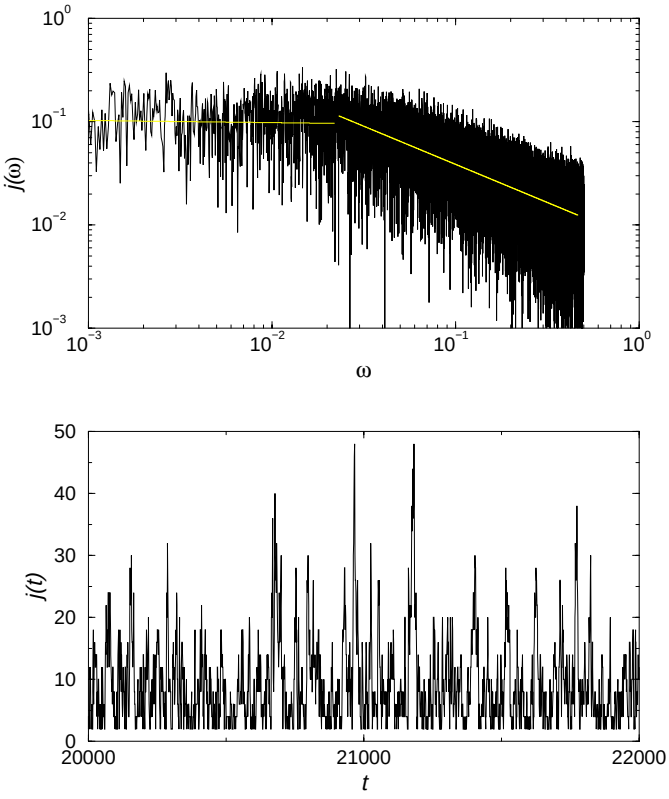

Fig. 2. Part of the switching current signal $j(t)$ against cumulative time t (lower panel) and the Fourier spectrum of the signal (top panel) for moderate pinning $f = 3.6$. Slope of the fitted area $\phi = 0.738 \pm 0.007$. Only nonzero values of current are shown (see text).

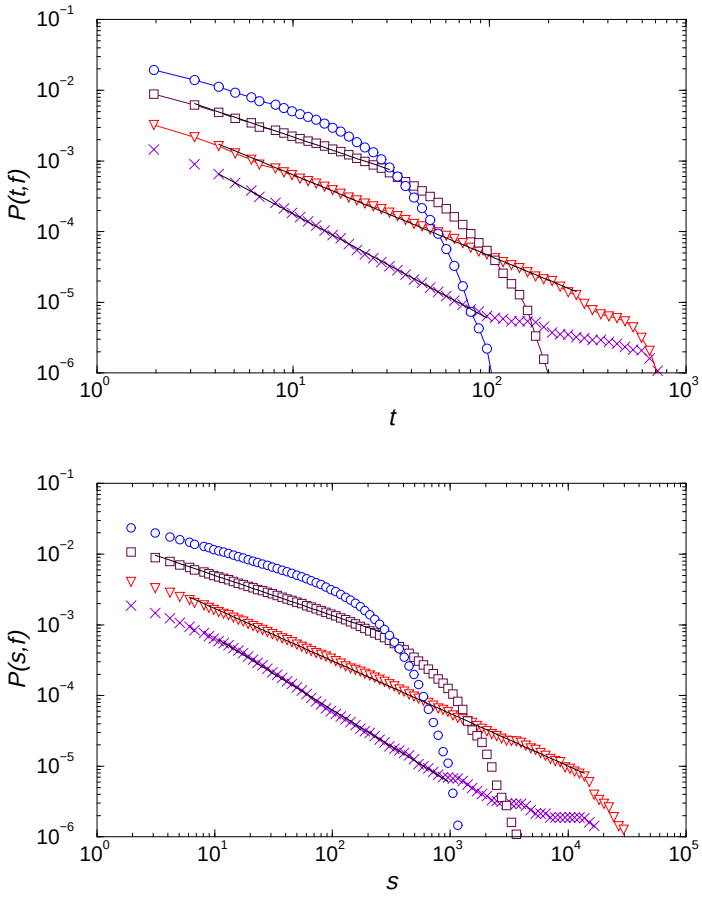

Fig. 3. Cumulative distributions of switched domain size $P(s,f)$ *vs.* size s (lower panel) and duration of switching $P(t,f)$ *vs.* duration t (top panel) for varying strength of pinning $f = 2.2$, 2.4, 2.8 and 3.2 (bottom to top, both panels). Driving rate is fixed $\Delta E/J = 0.001$. Fitted values of three slopes, corresponding to full lines, are (bottom to top): $\tau_s - 1 = 1.029(4)$, 0.747(2), 0.568(5), on the lower panel, and $\tau_t - 1 = 1.482(6)$, 1.145(7), and 0.94(2), on top panel. In total 4.32×10^6 spins divided into 20 different samples was used in simulations. Distributions are normalized by the actual number of avalanches during the full cycle and the number of samples. Data are log-binned with ratio 1.1.

depend on two relevant parameters – the domain size and the driving rate.

3.1 Varying strength of pinning

First we fix the driving rate to a small value $\Delta E/J = 1 \times 10^{-3}$ and consider how the domain size or strength of pinning influence the properties of the switching current. In Figure 3 we show the cumulative distributions of size (area) s of switched domains and duration t of switching following a single field update, for several values of pinning strength f. As the Figure 3 shows, both switched areas and durations of their switching show a wide range of values that are described by power-law distributions with finite cut-offs (X stands for $X \equiv s, t$):

$$P(X,L) = X^{-(\tau_X - 1)} \mathcal{P}\left(X L^{-D_X}\right). \qquad (3)$$

The scaling exponents $\tau_s - 1$ and $\tau_t - 1$ determine the respective slopes of the cumulative distributions of switched area and duration of switching (see Fig. 3). The fractal dimension D_s of size of switched domains and the dynamic exponent $D_t \equiv z$ in equation (3) determine how the corresponding cut-offs scale with the characteristic length (here the system size L), $X_0 \sim L^{D_X}$.

Both the slopes τ_X and the cut-offs, related to D_X, of the distributions depend on the strength of pinning. First, for weak pinning (small values of f, bottom curve in Fig. 3) we notice that extended domains, bounded by presumably plane domain walls, may occur. By increasing the field these domain walls move through a weakly random medium and eventually depin at a critical field $H_d(f)$. Depinning of large domain walls leads to a peak in the histogram at large values of s, or a plateau in the cumulative distribution as shown in Figure 3. Before the depinning is reached a series of small avalanches occurs that are power-law distributed. The plateau disappears at a critical value of pinning strength $f_c(r,L) \approx 2.4$, where a pure power-law distribution with virtually infinite cut-off (controlled only by the system size) occurs. Here the measured slopes give $\tau_s = 1.74$ and $\tau_t = 2.14$ for the fixed driving rate $\Delta E/J = 1 \times 10^{-3}$ (see Fig. 3).

At strong pinning (large f) many small domains are being nucleated at isolated points in the bulk and grow

Table 1. Scaling exponents for weak pinning ($f \approx f_c$) and for strong pinning ($f > f_c$) for 3-dimensional (3D) system at driving rate 4×10^{-4}, results of this work, and for 2-dimensional (2D) system at zero driving rate, from reference [28]. Estimated error bars are within ±0.03.

f (pinning)	Exponent	3D	2D
$f \approx f_c$	τ_s	1.78	1.54
(weak)	τ_t	2.20	1.83
$f > f_c$	τ_s	1.66	1.30
(strong)	τ_t	2.03	1.47

slowly along a few active sites per time step. The maximum sizes of domains are finite and decrease with stronger pinning (*cf.* top two curves in Fig. 3). Here the measured slopes give $\tau_s = 1.56$ and $\tau_t = 1.94$ for size and duration, respectively, suggesting another universality class of the scaling behavior, compared to the case of weak pinning. The transition to the strong pinning regime for $f > f_c$ is marked by disappearance of the critical depinning of large domain walls at all fields and domination of the nucleation processes. Numerical data in Figure 3 suggest that the critical value f_c is close to 2.4 for the used system size and driving rate.

Qualitatively similar behavior with two universality classes but with different exponents, was found in the case of two-dimensional system where an extended one-dimensional domain wall was initially prepared [28]. For comparison, in Table 1 we summarize exponents both for 3-dimensional and for 2-dimensional case. (Notice that the listed exponents for three-dimensional system are obtained for a small finite driving rate $\Delta E/J = 4 \times 10^{-4}$, whereas the simulations at zero driving rate were employed in two dimensions.) The results for 2-dimensional case are expected to be relevant for domains on the surfaces of the bulk samples (see Ref. [14]) and for thin films in which the width of the domain wall exceed the film thickness. An interesting physical realization of varying strength of pinning was suggested recently [29] in ferromagnetic $C_o/C_o O$ film by varying temperature through the transition temperature at which the substrate orders *anti*-ferromagnetically. As already mentioned, in ferroelectrics the local random fields are physical [13–16]. Therefore varying the strength of pinning due to random fields in ferroelectric thin films and bulk materials can be achieved in a more direct way, offering diverse possibilities to detect the change in the scaling behavior of the switching current noise and critical properties on the hysteresis.

3.2 Varying driving rate

In the following we examine how the scaling properties of the switching current noise change when the driving rate is increased. Very low frequencies of the driving field are usually not accessible on experiments, both for physical and technical reasons. A finite driving rate, which is defined as $r \equiv \langle \mathrm{d}E(t)/\mathrm{d}t \rangle$, can be approximated with $\Delta E/J$

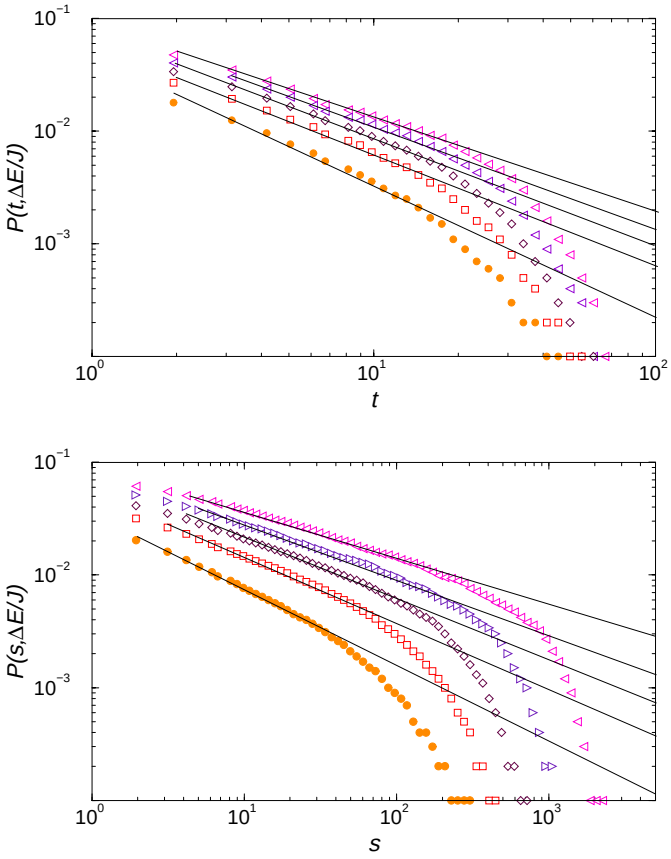

Fig. 4. Cumulative distributions of switched domain size $P(s, \Delta E/J)$ *vs.* s (lower panel) and duration of switching $P(t, \Delta E/J)$ *vs.* t (top panel) for fixed pinning $f = 3.2$ and varying driving rate $\Delta E/J = 4 \times 10^{-4}$, 1×10^{-3}, 2×10^{-3}, 4×10^{-3} and 8×10^{-3} (bottom to top on both panels). Normalization to the actual number of avalanches results in the vertical shift of the curves. Scaling region indicated by the section of the straight line. Log-binning ratio 1.1.

in the case of stepwise increase of the external field in the absence of back flips $b = 0$. For finite rate $r > 0$ the switching may start at different parts of the sample and the measured signal is a superposition of these separate events. In contrast to the mathematical limit of infinitely slow driving, by finite field jump ΔE the domain wall may get enough energy to overcome several pinning centers at the same time. Thus either different small domains are initiated simultaneously, or different parts of a large domain wall advance in parallel. In both cases the statistical properties of the signal are changed. Merging of many individual jumps makes the occurrence of large events more probable.

For a range of values of driving rates we still find a power-law behavior with reduced values of the scaling exponents and enlarged cut-offs. In Figure 4 we show how the distributions for sizes and durations of pulses vary when the driving rate $\Delta E/J$ is increased, while the strength of pinning was kept constant in the strong pinning regime. In Figure 5 the same type of analysis was done for the case of weak pinning. In the strong pinning

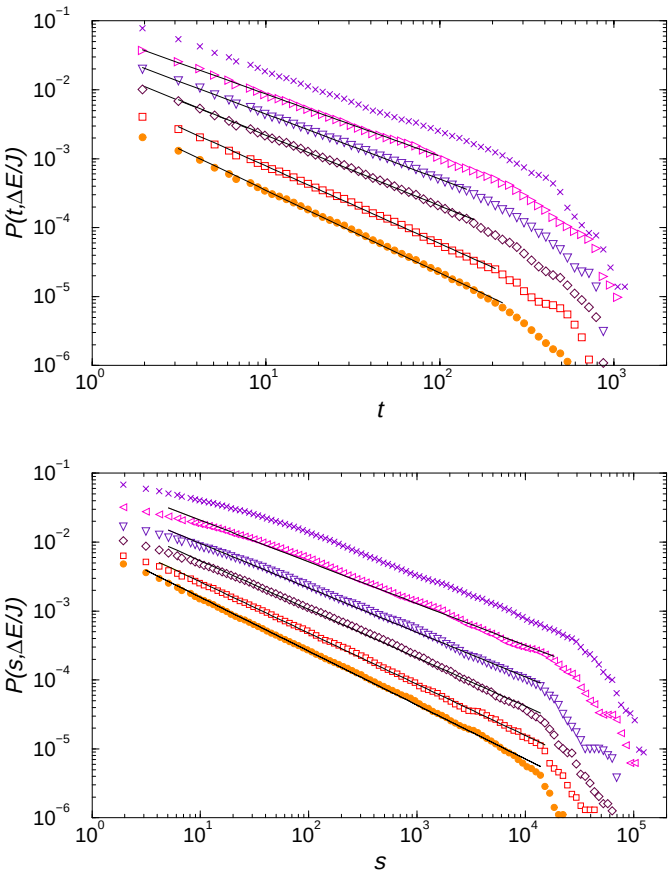

Fig. 5. Same as Figure 4 but for weak pinning regime $f = 2.4$. Driving rates are (bottom to top) $\Delta E/J = 4\times10^{-4}$, 1×10^{-3}, 2×10^{-3}, 4×10^{-3}, 8×10^{-3} and 1.2×10^{-2}. Fitted area on each curve is shown by solid line.

regime a dramatic increase of the cut-offs in the distribution of switched area occurs due to merging of many small signals. Whereas, in the weak pinning the relative enlargement of the cut-off is smaller, that can be understood as an effect of parallel advancement of different sections of the same extended wall, rather than merging of different domains. Both in strong and weak pinning case the increased incidence of large events leads to decrease of the scaling exponents. We find *logarithmic* dependence of the exponents for the size and duration of events on $\Delta E/J$ both in weak and strong pinning regimes. The results are shown in Figure 6 and the fit lines are given by the general form

$$\tau_X = A_X - B_X \ln(\Delta E/J). \qquad (4)$$

For the strong pinning both area and duration exponents decrease equally, *i.e.*, $B_s \approx B_t \approx 0.08$, with the constants $A_s \approx 1.0$ and $A_t \approx 1.4$. In the weak pinning, however, the duration exponent decreases with nearly double rate compared to the size exponent. We find $B_t \approx 2B_s \approx 0.11$, (see Fig. 6) and $A_t \approx 1.37$, $A_s \approx 1.30$ within numerical error bars.

It is important to note that the measuring conditions depend on the experimental set up and they can vary from

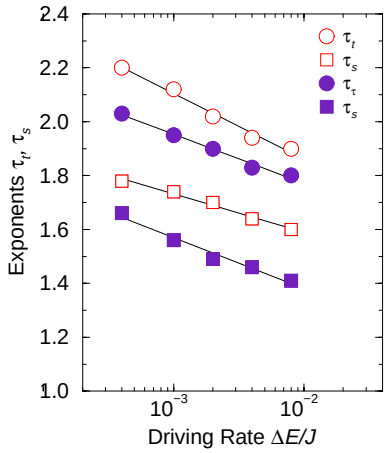

Fig. 6. Scaling exponents for the distribution of switched area (squares) and duration of pulses (circles) against driving rate $\Delta E/J$. Filled and open symbols correspond to strong and weak pinning, respectively. Fit lines: $\tau_X = A_X - B_X \ln(\Delta E/J)$, see text.

one experiment to the other. The effective driving rate depends on the steps in the external field and the degree of compensation of depolarization fields inside the sample. In real experiments the driving rate is always finite, resulting in the scaling exponents that are always *smaller* (and the fractal dimensions larger) compared to those computed in the theoretical limit of zero driving rate $r \to 0$. Therefore, in order to compare measured and predicted scaling exponents it is advisable to make several measurements at different driving rates and find out if the results, for instance for the area exponent τ_s, belong to a line in the range 1.66–1.40, which is compatible with occurrence of small domains, or in the range 1.78–1.60, suggesting that the sample has extended plane domain walls. When the driving rate is too large (*cf.* top line on both panels in Fig. 5), the scaling behavior of the distributions is lost. The cumulative probability distribution shows curvature both due to the lack of small events and the excess of large events.

4 Polarization reversal and back-switching

In the previous section we have shown how different kinds of domain walls in the sample determine the scaling properties of switching current noise, reflecting the nature of domain-wall motion when the electric field is slowly ramped. Here we consider another type of driving. First, in the initially polarized state (all spins down) we impose a large opposite field E_s and keep it until polarization reverses and reaches saturation in that field. Then we switch off the field to zero and monitor how the polarization decays. Both processes depend on the type of domains in the sample, and thus, on the strength of pinning. The results for polarization as a function of time are shown in Figure 7 for various strengths of pinning f.

For weak pinning spontaneous back switching of the polarization is exponentially fast, reaching the value P_r of

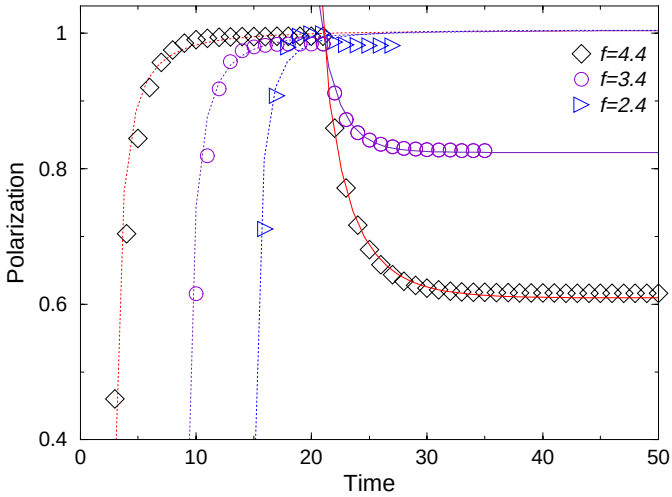

Fig. 7. Polarization reversal at field $E/J = 3$ (left part) and relaxation after field was set to zero (right part) against time for three values of pinning strength f, as indicated. Latter two lines were shifted to the right for better display. Fits according to $P = 1-C(t-a)^{-\nu}$ (dotted lines), and $P = A+B\exp[-(t/2-11)^{\sigma}]$ (full lines), see text.

remanent polarization. Whereas, the relaxation becomes increasingly slow as the strength of pinning f increases. The limiting values of P_r are lower, which correspond to increasingly slimmer loops for strong pinning (*cf.* form of the hysteresis loop in Fig. 1a). In general, polarization decay in Figure 7 can be approximated with a stretch exponential law $P(t) = A + B\exp[-(x/\tau)^{\sigma}]$, with $\sigma = \sigma(f)$ decreasing with the pinning strength. We have $\sigma \approx 1$, 0.92 and 0.80 for $f = 2.4$, 3.4, and 4.4, respectively. Qualitatively similar back-switching was recently observed in doped SBN: Ce^{3+} relaxor ferroelectric with two different stretching exponents corresponding respectively to illuminated and non-illuminated sample [15].

The polarization reversal in the strong constant field shows slow increase in the presence of small domains, but with another type of time dependence (see Fig. 7). The positive part of the polarization curve is fitted by the power-law increase $P(t) = 1 - C(t-a)^{-\nu}$, where $C \approx 0.8$, a is the respective shift (see Fig. 7) and the exponent $\nu \approx$ 2, 1.75, and 1.68, for $f = 2.4$, 3.4, and 4.4, respectively. Again, the characteristic exponent ν decreases when the pinning becomes stronger, thus contributing to the slow dynamics but within a power-law, rather than a stretch-exponential dependence.

5 Conclusions and discussion

We have shown that, in addition to the measurements of the hysteresis loop properties and smooth component of the switching current, the domain structure in a ferroelectric sample can be indirectly determined by the non-invasive dynamic measurements of the switching current noise and back-switching processes. Fractal character of the dynamic response indicates that a nontrivial domain structure can occur under slow field driving. The measured properties in these processes can be expressed in terms of universal exponents, which turn to be related in a unique way to the underlying structure and motion of domain walls. We have shown how the universal features of the switching current noise are quantified through two distinct sets of scaling exponents. The universal scaling behavior is associated with a dominant scenario of the domain wall dynamics: either the motion and depinning of large domain walls, in the case of weak pinning, or bulk nucleation and growth of many small 3-dimensional domains, in the case of strong pinning. The pinning in our model is provided by the local electric random fields.

Similarly, the polarization reversal in a strong applied field, and back-switching of the domains when the field is set to zero, are quick when large domains occurs, whereas they are slow when many small domains are nucleated. In the latter case the polarization relaxes according to a stretch-exponential law (the stretching exponent $\sigma < 1$) whereas it reverses with a fractal power of time (the characteristic exponent $\nu < 2$) when a large opposite field is switched on. In the case of weak pinning, on the contrary, the relaxation is exponential ($\sigma \approx 1$) and the reversal algebraic in time with $\nu = 2$. Dependence of the stretching exponent $\sigma(f)$ on the pinning strength is in qualitative agreement with measurements of back-switching in doped SBN: Ce^{3+} relaxor ferroelectrics [15], again suggesting that the local electric fields contribute significantly to slow the dynamics in this class of relaxors [15]. (Note that the characteristic time appears unrealistically small in our lattice model.) We are not aware of measurements of temporal behavior of the polarization reversal and of the switching current noise in these systems.

The observed scaling behavior of the switching current depends on the rate at which the driving field changes. We have demonstrated that in both universality classes the scaling exponents decrease *logarithmically* with increased driving rate $\Delta E/J$. This is in sharp contrast to the cases where the dominant type of disorder is due to random vacancies in spin-systems [4] and other avalanche-type dynamic systems driven at a finite rate [30], where the scaling exponents decrease and fractal dimensions increase *linearly* with the driving rate. Therefore, occurrence of the logarithmic dependences of the scaling exponents on the driving frequency may serve as an additional test of the presence of the real random fields in ferroelectrics.

Throughout this work we used the simulation algorithm at finite driving rates $\Delta E > 0$, that mimics the realistic situation in experiments. The obtained set of scaling exponents, together with their dependences on the driving rate, belongs to one (of the two) universality classes, which implies a definite domain structure of the system, and hence the expected character of the switching processes. Our results suggest that a crossover from one to the other universal behavior both in the switching current noise and in the polarization reversal and relaxation can be achieved by varying the strength of pinning due to random electric fields. As mentioned above, in practice there are various ways to accomplished the crossover by reducing

the pinning in ferroelectrics [9,15,27]. Here we have not discussed the properties of the dynamic phase transition separating these two scaling behaviors at a critical value f_c, nor the critical exponents describing the depinning transition along the critical field $H_d(f)$ for $f < f_c$. This questions require an additional study and proper finite size scaling analysis, for instance along the lines as done for the two-dimensional case in reference [28]. Finally, by allowing a frequent appearance of the unscreened depolarization fields a finite probability of negative pulses in the switching current builds up ($b \neq 0$). The presence of negative pulses slows the switching process, interferes with the effects of finite driving rates, and alters the scaling properties of noise. A more complete analysis of the switching processes for non-vanishing probability $b \neq 0$ is left for a future study.

Finally, it should be stressed that, in spite of its simplicity, the proposed model seems reasonable for dynamic properties of three-dimensional uniaxial relaxor ferroelectrics. Whereas, in the single-crystalline normal ferroelectrics a more realistic modeling of the effects of interactions and depolarization fields on domain structure is required. Nevertheless, we believe that, when restricted only to the *universal* scaling behavior of the noisy component of the switching current, the presented results for the case of large domains may not depend significantly on the details of interactions. Further research on the subject is necessary.

Work is supported by the Ministry of Education, Science and Sports of the Republic of Slovenia.

References

1. V.M. Rudyak, Usp. Fiz. Nauk **101**, 429 (1970)
2. E. Fatuzzo, W.J. Merz, *Ferroelectricity* (North-Holland, Amsterdam, 1967)
3. V.Ya. Shur, Phase Transitions **65**, 49 (1998)
4. B. Tadić, Physica A **270**, 125 (1999)
5. Dj. Spasojević *et al.*, Phys. Rev. E **54**, 2531 (1996)
6. L. Carillo *et al.*, Phys. Rev. Lett. **81**, 1889 (1998)
7. R.C. Miller, Phys. Rev. B **111**, 736 (1958); A.G. Chynoweth, J. Appl. Phys. **30**, 280 (1959)
8. V. Ya. Shur, E.V. Nikolaeva, E.L. Rumyantsev *et al.*, Ferroelectrics **222**, 323 (1999)
9. V. Ya. Shur, E.L. Rumyantsev, D.V. Pelegov *et al.*, Ferroelectrics (*Proceedings of IMF10*)
10. G. Pleyber *et al.*, Ferroelectrics **141**, 125 (1993)
11. E.V. Colla, L.K. Chao, M.B. Weissmann, Phys. Rev. Lett. **88**, 017601 (2002)
12. V. Ya. Shur, E.L. Rumyantsev, V.P. Kuminov *et al.*, Phys. Solid State **41**, 269 (1999); V. Ya. Shur, V.L. Kozhevnikov, D.V. Pelegov, *et al.*, *ibid.* **43**, 1128 (2001)
13. W. Kleemann, J. Dec, P. Lehnen *et al.*, Europhys. Lett. **57**, 14 (2002)
14. P. Lehnen, W. Kleemann, Th. Woike, R. Pankrath, Eur. Phys. J. B **14**, 633 (2000); Ferroelectrics **253**, 11 (2001); P. Lehnen, W. Kleemann, Th. Woike, R. Pankrath, Phys. Rev. B **64**, 224109 (2001)
15. T. Granzow, U. Dörfler, Th. Woike *et al.*, Europhys. Lett. **57**, 597 (2002)
16. A.P. Levanyuk, A.S. Sigov, *Defects and Structural Phase Transitions (Ferroelectricity and Related Phenomena)* (Taylor and Frances, London, 1988)
17. B. Tadić, Phys. Rev. Lett. **77**, 3843 (1996)
18. B. Tadić, Ferroelectrics **259**, 3 (2001)
19. E. Vives *et al.*, Phys. Rev. Lett. **72**, 1694 (1994)
20. O. Perković *et al.*, Phys. Rev. B **59**, 6106 (1999)
21. G.-P. Zheng, M. Li, Phys. Rev. B **63**, 36122 (2001)
22. Apart from weak pinning, more realistic interactions, *e.g.*, including elastic coupling are responsible for occurrence of the plane domain walls in normal ferroelectrics such as $BaTiO_3$
23. S. Sabhapandit, P. Shukla, D. Dhar, J. Stat. Phys. **98**, 103 (2000)
24. Notice that the properties of noise vary with the applied field, see for instance Refs. [8,12]
25. B. Tadić, Physica A **282**, 362 (2000)
26. R. Pirc, R. Blinc, Phys. Rev. B **60**, 13470 (1999); R. Blinc *et al.*, Phys. Rev. Lett. **83**, 424 (1999)
27. C.S. Lynch *et al.*, Ferroelectrics **166**, 11 (1995)
28. B. Tadić, U. Nowak, Phys. Rev. E **61**, 4610 (2000)
29. A. Berger *et al.*, Phys. Rev. Lett. **85**, 4176 (2000)
30. B. Tadić, V. Priezzhev, Phys. Rev. E **62**, 3266 (2000)